ADVANCED FUNCTIONAL MATERIALS
www.afm-journal.de

Photoclickable Surfaces for Profluorescent Covalent Polymer Coatings

*Mathias Dietrich, Guillaume Delaittre, James P. Blinco, Andrew J. Inglis, Michael Bruns, and Christopher Barner-Kowollik**

The nitrile imine-mediated tetrazole-ene cycloaddition reaction (NITEC) is introduced as a powerful and versatile conjugation tool to covalently ligate macromolecules onto variable (bio)surfaces. The NITEC approach is initiated by UV irradiation and proceeds rapidly at ambient temperature yielding a highly fluorescent linkage. Initially, the formation of block copolymers by the NITEC methodology is studied to evidence its efficacy as a macromolecular conjugation tool. The grafting of polymers onto inorganic (silicon) and bioorganic (cellulose) surfaces is subsequently carried out employing the optimized reaction conditions obtained from the macromolecular ligation experiments and evidenced by surface characterization techniques, including X-ray photoelectron spectroscopy and FT-IR microscopy. In addition, the patterned immobilization of variable polymer chains onto profluorescent cellulose is achieved through a simple masking process during the irradiation.

1. Introduction

A very simple technique to alter the surface properties of a bulk material is polymer coating. Often a covalent attachment is desirable to prevent dissolution of the coating in a solvent that the material could come in contact with. Polymer brushes are a particular class of covalent coating as they consist of chains individually linked to the substrate by single chemical bonds.[1] To covalently graft polymers to a surface, material scientists have two options. One can either grow the macromolecules from the surface (grafting from), or pre-synthesize the polymer and subsequently attach them by a chemical linkage (grafting to).[2] The first option usually yields higher grafting density since steric hindrance is rather low (only small monomeric molecules are added). Nevertheless, the second approach allows a full characterization of the polymer strands before grafting. If the chemical procedure employed to attach the polymer onto the surface is optimized (e.g., fast reaction times, high yield), a more efficient and homogeneous coverage of the surface can be obtained.[3] Several techniques have been established in the field of macromolecular science to fulfill these requirements. The combination of controlled/living radical polymerization (CRP)[4] and highly orthogonal and efficient conjugation reactions is a state-of-the-art example of precision chemistry giving control over material properties. In terms of CRP, the three main techniques entail nitroxide-mediated polymerization (NMP),[5] atom-transfer radical polymerization (ATRP),[6] and the reversible addition fragmentation chain transfer (RAFT) process.[7] All these methods have been applied synergistically with the concepts of click chemistry (introduced by Sharpless in 2001)[8] to produce a powerful toolbox for the synthesis of materials with tailored macromolecular architectures.[9] Numerous modular ligation reactions – some of which adhere to the click criteria – have been successfully applied to polymer chemistry and surface grafting.[10] An important fraction of the reported studies involves the use of copper or other metal catalysts. When working with biological systems, the use of metal catalysts should preferentially be avoided due to their potential cytotoxicity.[11] Recently several metal-free techniques have been applied to polymeric materials to address this issue.[12] Particularly, few modular ligation reactions feature a light-triggered activation process, e.g., thiol-ene and thiol-yne radical additions when performed in the presence of a photoinitiator[13] or the UV-light-triggered Diels–Alder reaction between

M. Dietrich, Dr. G. Delaittre, Dr. J. P. Blinco, Dr. A. J. Inglis, Prof. C. Barner-Kowollik
Preparative Macromolecular Chemistry
Institut für Technische und Polymerchemie
Karlsruhe Institute of Technology (KIT)
Engesserstr. 18, 76128 Karlsruhe, Germany
E-mail: christopher.barner-kowollik@kit.edu
M. Dietrich
Environmental Engineering Group
Fraunhofer Institute of Chemical Technology
Joseph-von-Fraunhofer-Str. 7, 76327 Pfinztal, Germany
Dr. G. Delaittre
Zoologisches Institut
Zell- und Neurobiologie
Karlsruhe Institute of Technology (KIT)
Haid-und-Neu-Straße 9
76131 Karlsruhe, Germany
Dr. M. Bruns
Institute for Applied Materials (IAM-WPT) and Karlsruhe Nano Micro Facility (KNMF)
Karlsruhe Institute of Technology (KIT)
Hermann-von-Helmholtz-Platz 1
76344 Eggenstein-Leopoldshafen, Germany

DOI: 10.1002/adfm.201102068

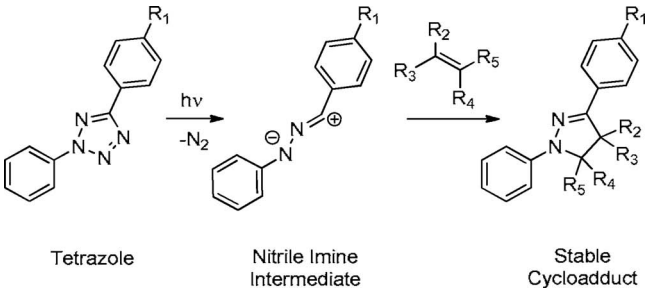

Scheme 1. Schematic representation of the UV-induced formation of the nitrile imine from a tetrazole and its subsequent 1,3-dipolar cycloaddition with dipolarophiles.

2,5-dimethylbenzophenone derivatives and maleimides introduced by our team.[14] Using light as a trigger additionally provides temporal and spatial control of the reaction.

Recently, Lin and co-workers[15] re-discovered a light-induced ligation methodology based on the nitrile imine-mediated 1,3-dipolar cycloaddition of a tetrazole and an ene (NITEC) which was first reported by Huisgen and Sustmann[16] in 1967 and has been very rarely employed since.[17] Starting with a tetrazole-containing compound, the reaction is initiated by UV irradiation. Upon light exposure, nitrogen is released from the molecule and a reactive nitrile imine moiety is formed in situ (see **Scheme 1**). Nitrile imines have been shown to readily undergo reactions with various electron-deficient and unactivated terminal alkenes and alkynes to form a stable pyrazoline-based covalent linkage.[15a,b,18] Compared to other, more established modular ligation reactions, NITEC presents several advantages such as: i) simplicity of implementation since tetrazole-based molecules are rather facile to synthesize and only a simple hand-held UV lamp is required for activation due to high photolysis quantum yields, ii) the absence of a metal catalyst, iii) fast reaction times, and iv) bio-orthogonality. For instance, it was possible to functionalize chemically modified[15c] or genetically engineered[19] enzymes in vitro, as well as a genetically engineered protein directly in *Escherichia coli*[20] or – even more impressively – stabilize the helical structure of a peptide by intramolecular NITEC-stapling.[21] The aim of our current work is to introduce the NITEC approach to the field of soft matter material science and to demonstrate its potential for the rapid covalent coating of (bio)surfaces with macromolecules, in order to modify their physical properties.

The current study is divided into three distinct, yet complementary sections. Initially, we evaluate the possibility of employing the NITEC approach for macromolecular conjugation as the products of the reaction can be analyzed by simple solution characterization techniques. Once optimum coupling conditions are identified, grafting of a hydrophobic polymer onto silicon wafers is undertaken. Finally, the power of the NITEC technique to modify biosurfaces is demonstrated by the grafting of variable functional macromolecules onto cellulose membranes to generate fluorescent (patterned) surfaces.

2. Results and Discussion

2.1 Macromolecular Conjugation

While the NITEC approach has been successfully applied to the conjugation of a number of small molecules or small molecules with proteins as well as for the PEGylation of proteins,[15–22] the technique has never been applied for the linking of two synthetic macromolecules or the attachment of a polymer to a surface. To evaluate the applicability of NITEC in macromolecular chemistry, model conjugation experiments were conducted. **Scheme 2** depicts the synthetic pathway for the formation of diblock copolymers from tetrazole- and maleimide end-functionalized polymers, respectively. In the current study, the tetrazole and the maleimide moieties were installed on poly(ethylene glycol) methyl ether (PEG) by esterification. Using DCC coupling, tetrazole-bearing PEG **1** and maleimide-terminated PEG **2a** could be synthesized in close-to-quantitative yields with end-group functionality confirmed via electrospray ionization coupled to mass spectrometry (ESI-MS) (see Figure S3 and S4). Maleimide was chosen as the

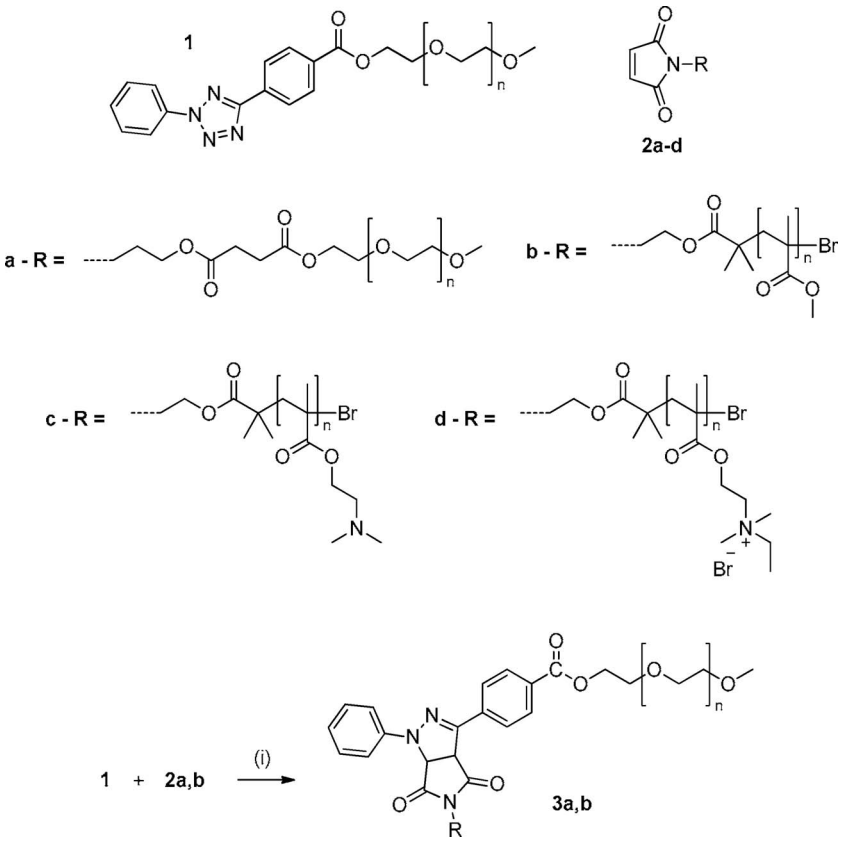

Scheme 2. Tetrazole- (**1**) and maleimide-functionalized (**2a–d**) polymers employed in the current study and their model macromolecular conjugation reactions. (i) ethanol, $h\nu = 254$ nm.

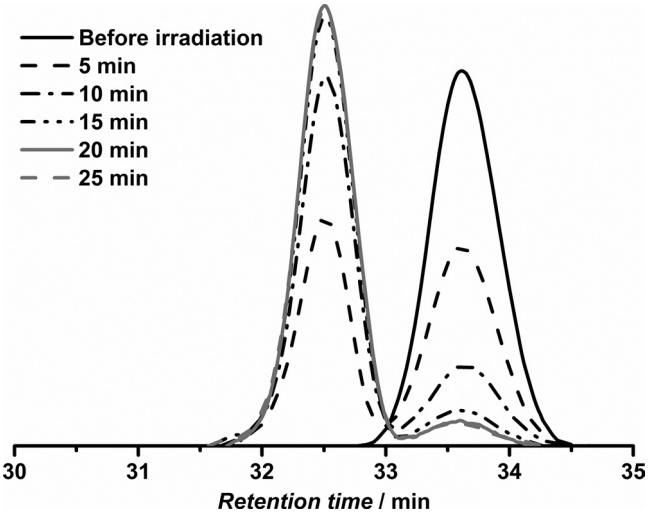

Figure 1. SEC monitoring of the poly(ethylene glycol)-*block*-poly(ethylene glycol) copolymer formation after irradiation of an equimolar solution of **1** and **2a** in ethanol with a hand-held UV lamp at a wavelength of 254 nm at ambient temperature. See Scheme 2 for the chemical structures underpinning the transformation.

dipolarophile end group as it has been shown to undergo rapid reaction with nitrile imine intermediates.[15a,b,18] Furthermore, in addition to the postpolymerization approach, an ATRP functional initiator can also be employed to readily introduce a maleimide moiety onto the terminus of a wide range of polymers.[23] We followed this procedure to produce α-maleimido poly(methyl methacrylate) (PMMA) (**2b**) and poly(dimethylaminoethyl methacrylate) (PDMAEMA) (**2c**).

To assess the conjugation efficiency of the NITEC process, equimolar amounts of PEG-tetrazole **1** and PEG-maleimide **2a** were dissolved in ethanol and subsequently irradiated at 254 nm employing a hand-held laboratory TLC lamp. **Figure 1** shows the size-exclusion chromatograms of samples withdrawn after variable irradiation times and left to stand overnight. The success of the conjugation is evidenced by a distinct shift of the SEC traces to shorter retention time due to the formation of higher molecular weight polymer. The intensity of the initial low molecular weight polymer decreases progressively with the increase of intensity of the peak at higher molecular weights, which evidences the formation of block copolymers starting from homopolymer precursors. Indeed, the observed evolution differs completely from what can be observed when a block copolymer is produced by the extension of a reactive polymer with iterative addition of monomer, i.e., a progressive shift of the entire SEC signal in the ideal case. The final product exhibits a molecular weight of 4300 g mol^{-1}, which is approximately the double of that of the starting compounds (M_n = 2200–2300 g mol^{-1}) as expected in the case of a quantitative conjugation. A closer look at the intermediate samples reveals that after only 5 min of UV irradiation (at ambient temperature) half of the starting materials had already reacted, and after 10 min less than 20% remained. No significant difference could be observed between samples taken after 15, 20, or 25 min. The remainder of a very minor amount of starting material could be explained by a nonquantitative functionalization during the synthesis of **1** and/or **2b**. It is important to note that a perfectly equimolar solution of starting material is not easy to prepare when one works with macromolecules, owing to their polydispersities and thus chain distribution character.

It is further interesting to note that during and after the successful copolymer formation a strong fluorescence of the generated copolymers can be observed, even in the solid state. This fluorescence arises from the newly formed diaryl-Δ^2-pyrazoline which, although it does not present any continuous conjugation in the classical sense, possesses two mesomeric canonic forms allowing the two aromatic rings to interact.[24] The fluorescence is thus only observed in samples where successful coupling has occurred. When the tetrazole was irradiated for long periods in the absence of a dipolarophile, no fluorescence was observed. The formation of AB-type block copolymers between PEG-tetrazole **1** and maleimide-PMMA **2b** additionally proved to proceed in a similar manner (see Figure S6).

2.2. Grafting of Polymers onto Silicon Wafers via NITEC

After the successful ambient temperature coupling of two polymer chains, the grafting of polymers onto an inorganic surface was examined. Initially, silicon wafers were chosen as substrates due to their ease of characterization with techniques such as X-ray photoelectron spectroscopy (XPS). For this purpose, a tetrazole-containing silane was synthesized for covalent attachment to the surface of the wafers (see **Scheme 3** and the Supporting Information). The functionalization was realized by heating a cleaned and activated silicon wafer in a silane solution, yielding a polysiloxane multilayer coating with covalently bound tetrazole moieties. The tetrazole-functionalized silicon wafer was cleaned extensively after the reaction by rinsing with fresh solvent and ultrasonification to remove any physisorbed tetrazole silane from the surface. **Figure 2**a displays the C 1s and N 1s regions of the XPS spectra of the silicon wafer after tetrazole functionalization. The spectra were normalized to the peak with the highest intensity. The main peak in the C 1s spectrum at 285.0 eV is assigned to saturated carbon atoms (C–C, C–H) and is employed as a reference to compare the evolution of the different carbon species present on the surface. The peak at 286.7 eV is assigned to carbon atoms involved in various single bonds with oxygen and nitrogen (C–O, C–N), while the peak at 288.6 eV is assigned to the carboxyl group (–O–C=O).[25,26] The N 1s spectrum shows a strong peak at 400.4 eV that can be assigned to the tetrazole species (–N=N–)[27] while the additional weak N 1s component at 402.4 eV (probably positively charged nitrogen) cannot be assigned unambiguously.[28]

Nitrile imines have mostly been considered as transient intermediates and are not easy to observe.[18a] It has already been shown that a nitrile imine very similar in structure to the one generated in our study can be trapped by nucleophilic addition of ethanol or water to form a hydrazone or a hydrazide, respectively.[29] To assess the possibility of such a reaction, wafer **4** was irradiated in ethanol in the absence of any dipolarophile (Figure 2b). The XPS results are in rather good agreement with the assumption that these reactions occur (see Figure S8 and S9). Indeed, for a constant carbon concentration, the nitrogen content is more than halved while the concentration of heteroatom-bound carbon slightly increases.

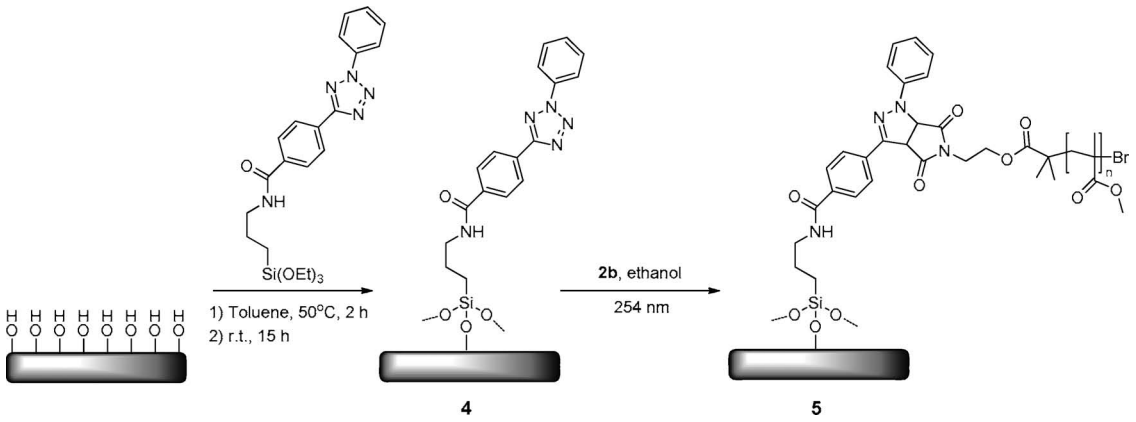

Scheme 3. Synthetic route for the formation of poly(methyl methacrylate)-grafted silicon wafers.

Although the nucleophilic addition can theoretically take place as demonstrated above, it must be noted that in the presence of a dipolarophile the NITEC is much more rapid and proceeds in a quantitative fashion.[17b] Nevertheless, this control experiment evidences the release of nitrogen from the surface, and the formation of nitrile imine moieties. To graft a maleimide-functionalized polymer, a similar methodology as described above for the block copolymer formation was employed for the NITEC reaction on the silicon surface. Wafer **4** was placed in a solution of **2b** in ethanol, irradiated for 15 min and subsequently left to stand in the polymer solution for a further 45 min (Scheme 3). Sample **5** was then investigated by XPS after extensive rinsing with fresh solvent (Figure 2c). In comparison to the unreacted tetrazole-containing wafer **4** (Figure 2a), **5** contains 2.8-fold and 7.8-fold greater amounts of saturated and unsaturated carbons atoms, respectively, bound to a nitrogen or an oxygen atom. This result evidences the presence of the methacrylic polymer **2b** on the surface. The magnitude of the increase for these particular XPS signals is in the range expected for a close-to-quantitative grafting (see the Supporting Information, Section 2.3). However, the expected bromine content is below the detection limit of XPS and it is impossible to distinguish between nitrogen attributed to tetrazole and imide/amide, respectively.[30] Compared to unmodified silicon wafers or control experiments where either the tetrazole or the polymer was missing, the overall spectrum displays a decrease of the substrate silicon peak (ca. 25% of its initial value) due to the formation of a thicker hydrocarbon layer on the surface and corroborates the success of the surface functionalization (data not shown).

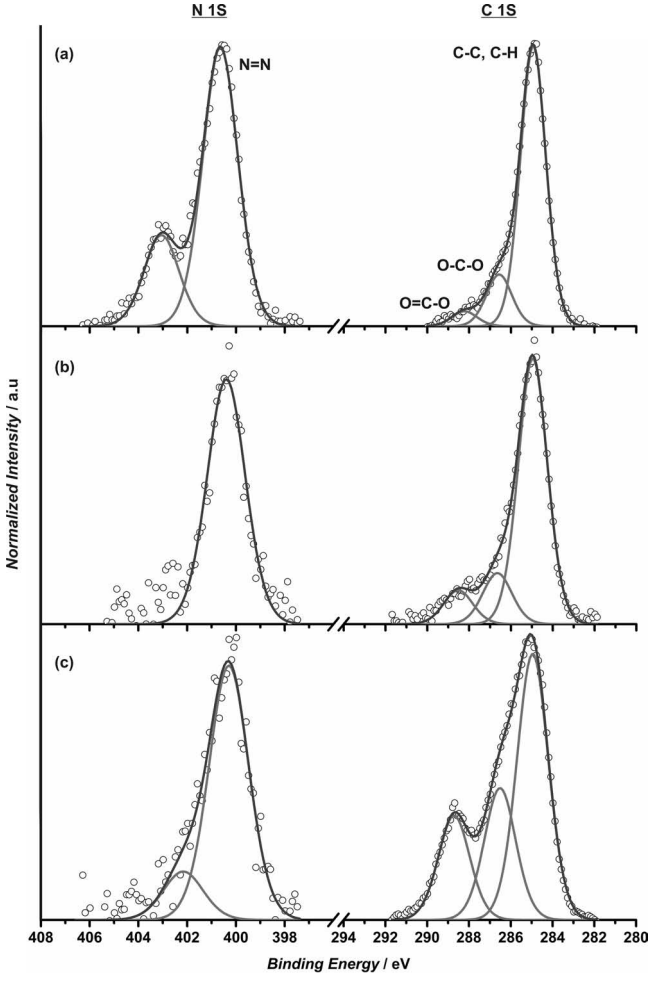

Figure 2. Comparison of the N 1s and C 1s normalized regions of XPS spectra of wafer **4** (a), wafer **4** irradiated for 15 min at 254 nm (b) and wafer **5** (c). All spectra are normalized to maximum intensity.

2.3. Grafting of Polymers onto Cellulose via NITEC

The successful grafting onto silicon wafers prompted us to investigate the functionalization of a more complex system. We chose cellulose as a wide-range-application biosubstrate.[31] Cellulose membranes were immersed in a 10 wt.% sodium hydroxide solution to break down the extensive hydrogen bonding due to the numerous hydroxyl groups and to open any crystalline regions in order to increase the availability of these free hydroxyl groups at the surface (**Cel–OH**). The carboxy-containing tetrazole previously employed for the synthesis of **1** was covalently bound to the cellulose by esterification of the primary alcohol present on the repeating sugar unit to give **Cel–Tet** (**Scheme 4**).

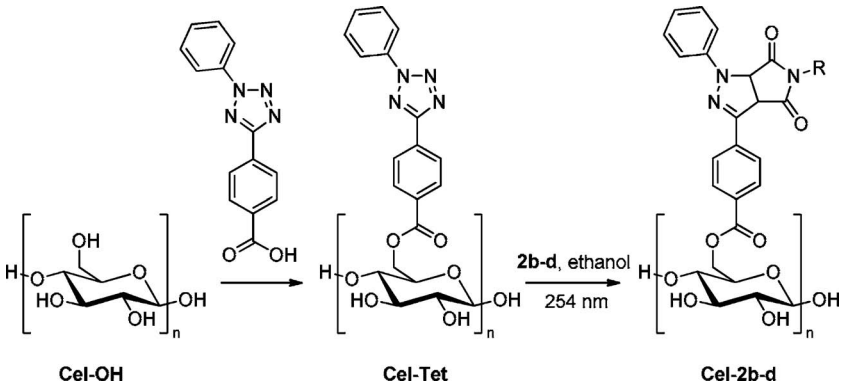

Scheme 4. Strategy for surface modification of cellulose by NITEC through esterification of cellulose with carboxyl-functionalized tetrazole and subsequent photografting of polymers **2b–d**.

After thorough rinsing, the treated cellulose **Cel–Tet** was analyzed by XPS (**Figure 3**). Contrary to silicon wafers, cellulose is a fibrous material and is thus intrinsically heterogeneous. Consequently, when the surface modification consists in the grafting of a small molecule, it is challenging to draw conclusive interpretation and almost impossible to predict theoretical values of atomic contents. However, observation of the evolution of the different species can still be useful. Indeed, while no signal was detected in the N 1s region of the XPS spectrum of **Cel–OH** (Figure 3a), a low-intensity peak could be observed for **Cel–Tet** at 400.4 eV (Figure 3b), which is indicative of the nitrogen-containing tetrazole being present. On the contrary, it is not possible to evaluate the C 1s region since the cellulose signals are very strong in this region and prevent any accurate detection of a contribution – which would be very low – from the tetrazole handle. While the weak contribution at 285.0 eV (C–C, C–H) is caused by hydrocarbon contamination, it must be noted that carbonyl groups can be detected in **Cel–OH** and originate from oxidation that can readily occur on natural fibers such as cellulose.[32] The tetrazole-functionalized cellulose was subsequently immersed in a solution of **2b** in ethanol and irradiated at 254 nm at ambient temperature for 10 min on each side and left to stand in the polymer solution for a further 50 min before being washed with different solvents and dried under vacuum. XPS data support the formation of a grafted (meth)acrylic polymer layer as shown in Figure 3c. Indeed, in comparison to the cellulose characteristic peaks, a clear increase of the C–C/C–H signal (285.0 eV) is observed on one hand and of the O=C–O signal (289.2 eV) on another hand. Within the experimental uncertainties, all measured binding energies are similar to those found for the Si-system. However, due to the high cellulose background one cannot directly compare **Cel–2b–d** with sample **5** (Scheme 3, Figure 2c).

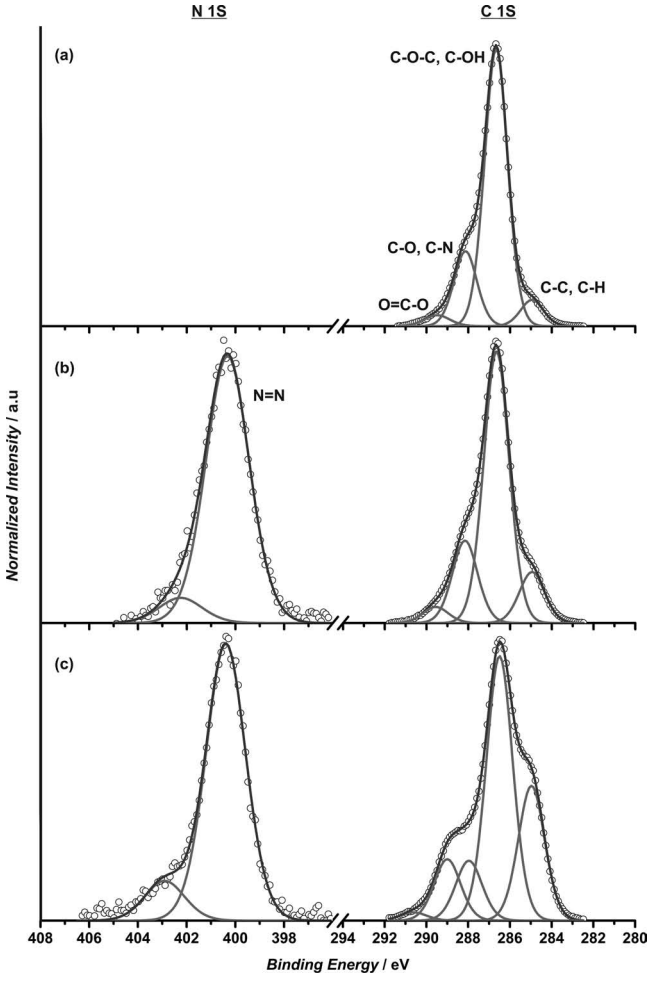

Figure 3. Comparison of the N 1s and C 1s normalized XPS spectra of **Cel–OH** (a), **Cel–Tet** (b), and **Cel–2b** (c). All spectra are normalized to maximum intensity.

As a complementary surface characterization technique we additionally employed Fourier-transform (FT-IR) microscopy, which allows a high-resolution spatial chemical mapping. We already demonstrated that FT-IR microscopy was efficient to prove the grafting of polymer chains onto cellulose by an acid catalyzed hetero-Diels–Alder ligation reaction.[33] **Figure 4** shows the false-color, high-resolution FT-IR microscopy images of the PMMA-grafted cellulose and of the control sample in which **Cel–Tet** was immersed in a solution of **2b** but not irradiated. Figure 4a and c show the integration range corresponding to the characteristic cellulose signals of the C–O stretching vibration (950–1200 cm^{-1}) and therefore represent a cellulose fiber. Figure 4b and d show the carbonyl spectral region (1675–1765 cm^{-1}), corresponding to PMMA lateral ester groups. The sample obtained from the reaction of **2b** with the tetrazole-functionalized cellulose is clearly much richer in carbonyl groups (Figure 4b) than the control sample, where no distinguishable peak is visible (Figure 4d). Although a carbonyl bond is introduced onto the cellulose after the tetrazole functionalization, it is not visible as its amount is too low to be detected with the focal plane array detector. This result corroborates the attribution of the carbonyl bonds observed in Figure 4b to the presence of the polymer on the surface of the cellulose fibers and proves that no polymer is physically adsorbed to the surface.

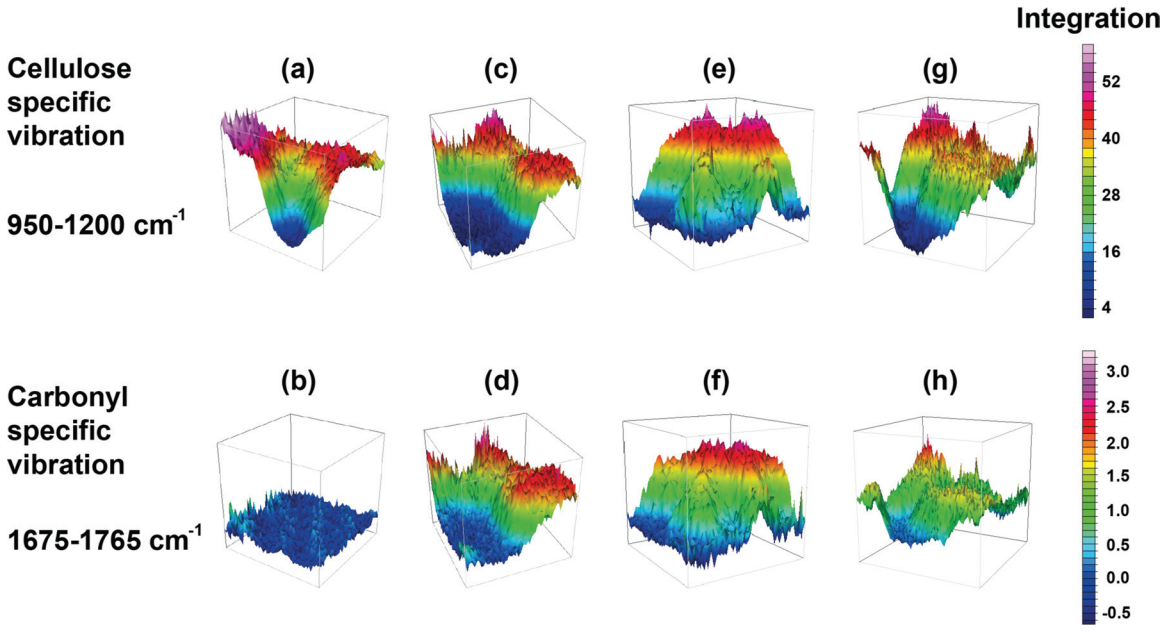

Figure 4. False-color high-resolution FT-IR microscope images (4 cm^{-1} spectral resolution with a 0.25 μm^2 spatial pixel resolution and an optical resolution of close to 1 µm) of the different cellulose samples. Top row: Integration between 950 and 1200 cm^{-1}. Bottom row: Integration between 1675 and 1765 cm^{-1}. a,b) **Cel–Tet** after immersion in a solution of **2b** without being irradiated; c,d) **Cel–2b**; e,f) **Cel–2c**; g,h) **Cel–2d**. Cellulose regions with green to pink color correspond to an increasing functionality within the particular integrated wavelength region.

In direct support of the macromolecular conjugation experiments, the appearance of fluorescence provides a direct visualization method to assess the success of the grafting reaction. Indeed, all the samples which proved to have been functionalized when analyzed by XPS or FT-IR microscopy exhibited fluorescence. To demonstrate that the light-triggered nature of the NITEC method could certainly be employed to precisely pattern surfaces, we performed the same reaction as above but irradiating a tetrazole-functionalized cellulose membrane which had been partially masked. The clear difference under a 366-nm light between the irradiated and the masked parts of the cellulose is evidenced on **Figure 5**a. Submitting this piece of cellulose to XPS showed that the masked and the irradiated parts had spectra comparable to that of the initial tetrazole-functionalized cellulose **Cel–Tet** and the PMMA-grafted cellulose **Cel–2b**, respectively.

An additional proof that polymer grafting only occurred on the non-masked part is provided by the change of physical properties due to the presence of a hydrophobic polymer such as PMMA on the surface. Figure 5b depicts a **Cel–2b** sample where a water droplet has been placed. While the droplet can be observed on this irradiated sample for several tens of minutes without any drastic change, a similar experiment with a control sample (**Cel–Tet** placed in a solution of **2b** but not irradiated) led to instantaneous absorption of the droplet. Additionally, water contact-angle measurements were carried out. Due to the inherent roughness and adsorbing nature of the cellulose surface, such a measurement is not straightforward. Indeed, it is generally very difficult to obtain a value for the pristine cellulose due to the aforementioned fast absorption. However, in the present case, the control sample is not native cellulose but tetrazole-functionalized **Cel–Tet**. The non-changed wetting behaviour when going from the virgin cellulose to **Cel–Tet** is rather interesting, since it shows that before the polymer grafting, the sample properties are not drastically altered by

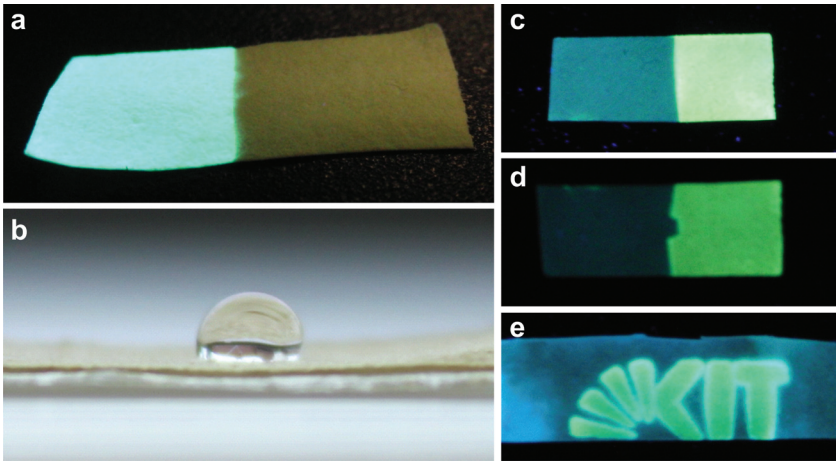

Figure 5. a) Photograph under 366-nm UV light of a piece of cellulose after irradiation of its left half at 254 nm in an ethanol solution containing **2b**. b) Photograph of a water droplet 10 min after its deposition on a piece of cellulose **Cel–2b**. c–e) Photographs of pieces of cellulose under a 366-nm light after a 10-min-per-side irradiation at 254 nm, on their right-hand half in ethanol solutions containing **2c** (c) and **2d** (d) and using a hand-made aluminum foil KIT mask in an ethanol solution containing **2b** (e).

the tetrazole functionalization. On the contrary, the part which was irradiated in the presence of **2b** became very hydrophobic exhibiting a water contact angle of 126°.

In addition to the grafting of a hydrophobic polymer and to evidence the power of the combination of modern polymer chemistry and NITEC to yield functional materials, we also carried out the covalent coating of the thermo- and pH-sensitive polymer **2c** and the antibacterial polymer **2d**,[34] as evidenced by FT-IR microscopy. Indeed the reaction proved to proceed as in the case of the grafting of **2b**, i.e, intense signals in the carbonyl spectral region (1675–1765 cm^{-1}) were observed (Figure 4e–h for the grafting of **2c** and **2d**, respectively). Similarly, simple fluorescence observation revealed the presence of the pyrazoline linkage (Figure 5c and d, respectively). Finally, the patterning ability offered by the NITEC process was evidenced by the use of a slightly more complicated mask representing the KIT logo. Figure 5e depicts the patterned covalent coating of maleimido-PMMA **2b** on tetrazole-functionalized cellulose. Obviously only the irradiated areas exhibit fluorescence and prove the spatially defined localization of pyrazoline-linked PMMA on the cellulose.

3. Conclusions

The UV-induced formation of nitrile imines from tetrazoles and its subsequent 1,3-dipolar cycloaddition with maleimides was successfully employed for the efficient ambient temperature modular ligation of polymer chains as well as their grafting to surfaces such as silicon or cellulose. As the reaction requires irradiation by UV light to be initiated, a spatially defined polymer grafting can be achieved. The reaction works very rapidly under non-demanding conditions and can be applied to a number of polymers due to the ease of the introduction of alkene end groups onto synthetic macromolecules, yet also to many different surfaces provided that the tetrazole moiety can be anchored. An additional exceptional advantages of the NITEC technique are the absence of necessary purification (the only by-product is molecular nitrogen), its profluorescent character allowing a rapid assessment of its success as well as its already-proven bioorthogonality. Compared to other more established modular ligation reactions, the NITEC approach has a great potential for bioorthogonal macromolecular conjugation and soft matter material design. Efforts in our lab are currently directed towards the application of the technique in nanobiotechnology.

4. Experimental Section

All experimental details pertaining to organic and macromolecular synthesis procedures are reported in the Supporting Information section. All surface-related synthetic and analytic procedures are reported in the following.

Functionalization of Silicon Wafers with Tetrazole: Three activated silicon wafers (0.8 × 0.8 cm) were placed in a 10 mL round bottom flask containing a solution of carboxy-functionalized tetrazole in dry toluene (9.6 mg in 2 mL). The flask was heated to 50 °C for 2 h and subsequently left to stand at ambient temperature for another 15 h, after which the wafers were rinsed thoroughly with fresh toluene and sonicated 15 min in toluene plus 5 min in acetone. The wafers were finally dried in a stream of nitrogen.

Polymer Photografting onto Silicon Wafers: The wafers were introduced into separate quartz cuvettes containing a solution of **2b** (25 mg) in ethanol (1 mL), irradiated for 10 min and left to stand in the solution for further 45 min. The wafers were subsequently extensively rinsed with fresh ethanol and acetone. For the control experiments, either no polymer was present or no irradiation was performed.

Functionalization of Cellulose with Tetrazole: Cellulose consists of D-anhydroglucose units joined together by β-1,4-linkages.[35] In their native state, cellulose chains feature strong intermolecular hydrogen bonding due to the hydroxyl groups. Prior to surface modification, cellulose substrates were thus subjected to a pretreatment: the cellulose sheets were immersed in an aqueous solution of 10 wt% NaOH to break down the extensive hydrogen bonding between the OH groups and to open up the ordered regions so that the reagents can penetrate more readily into the cellulose substrate and render it accessible for further modification. They were subsequently washed thoroughly with ethanol, dichloromethane (DCM) and finally with dry DCM. Prior to the reaction with cellulose, the carboxy-functionalized tetrazole was turned into its more reactive acyl chloride counterpart: carboxy-functionalized tetrazole (110 mg, 0.41 mmol) was dissolved in dry DCM (10 mL) with a catalytic amount of dry *N,N*-dimethylformamide (DMF) and oxalyl chloride (140 µL, 1.63 mmol) was added dropwise and reacted for 10 h. Excess oxalyl chloride was subsequently removed under reduced pressure. The acid chloride-functionalized tetrazole was redissolved in DCM (2 mL) and added dropwise to a suspension of freshly NaOH-treated cellulose (3 pieces, 0.8 × 1.5 cm each) in DCM (5 mL) containing DMAP (26 mg, 0.21 mmol) and DIPEA (0.7 mL. 4.02 mmol). After 10 h reaction time, the functionalized cellulose was washed extensively with ethanol, acetone, and DCM and finally stored in pure ethanol away from light.

Polymer Photografting: The pieces of cellulose were placed into separate quartz cuvettes containing a solution of **2b**, **2c**, or **2d** (20 mg) in ethanol (1 mL). The samples were subsequently irradiated for 10 min on each side on the cellulose sheets and left to stand in the solution for another 50 min. Subsequently the cellulose samples were rinsed extensively with ethanol, acetone, and water before being dried overnight in a vacuum oven at 40 °C. For the control experiments, either no polymer was present or part of the samples were protected from irradiation (masking technique).

X-ray Photoelectron Spectroscopy: Investigations were performed on a K-Alpha spectrometer (ThermoFisher Scientific, East Grinstead, U.K.) using a microfocused, monochromated Al Kα X-ray source (200 µm spot size). Up to 30 separated spots were measured to prevent the samples from X-ray damage, each at minimum acquisition time. All spectra were finally collapsed to one single spectrum with a sufficient signal/noise ratio. The kinetic energy of the electrons was measured by a 180° hemispherical energy analyzer operated in the constant analyzer energy mode (CAE) at 50 eV pass energy for elemental spectra. The photoelectrons were detected at an emission angle of 0° with respect to the normal of the sample surface. The K-Alpha charge compensation system was employed during analysis, using electrons of 8 eV energy and low-energy argon ions to prevent any localized charge build-up. Data acquisition and processing using the Thermo Avantage software is described elsewhere.[36] The spectra were fitted with one or more Voigt profiles (BE uncertainty: (±0.2 eV). The analyzer transmission function, Scofield sensitivity factors,[37] and effective attenuation lengths (EALs) for photoelectrons were applied for quantification. EALs were calculated using the standard TPP-2M formalism.[38] All spectra were referenced to the C1s peak of hydrocarbon at 285.0 eV binding energy controlled by means of the well-known photoelectron peaks of metallic Cu, Ag, and Au, respectively.

FT-IR Microscopy Imaging: Infrared measurements of the cellulose samples have been performed using a Bruker FT-IR microscope HYPERION 3000 coupled to a research spectrometer VERTEX 80. The HYPERION 3000 microscope is equipped with a multi-element FPA-detector (focal plane array) for imaging, which was used for laterally resolved measurements. The multi-element FPA-detector consists of 64 × 64 elements. This allows for the simultaneous acquisition of 4096 spectra covering a sample area of 32 × 32 µm (for ATR detection). With the FPA-detector in combination with the 20× Germanium ATR-lens, a

lateral resolution of 0.25 μm^2 per pixel is achieved. This high resolution is needed for the analysis of single fibers within the cellulose matrix to examine the homogeneity of the covalent functionalization applied on the cellulose. Besides the high lateral resolution, the extremely short measurement time (<2 s per scan) is another significant benefit of the FPA-detector. With the FPA-detector, 4096 spectra are acquired simultaneously within a few seconds. For postprocessing a baseline correction and atmospheric compensation were used.

Contact-Angle Measurements: The water contact angle of **Cel–2b** was determined by the sessile drop method using a Krüss DSA 100 contact angle meter for measurement and the Krüss DSA 2 software for analysis. The water droplet volume was 4 µL.

Supporting Information

Supporting Information is available from the Wiley Online Library or from the author.

Acknowledgements

C.B.-K. acknowledges continued financial support from the Karlsruhe Institute of Technology (KIT) in the context of the Excellence Initiative for leading German universities as well as the German Research Council (DFG) and the Ministry of Science and Arts of the State of Baden-Württemberg. M.D. thanks the Fraunhofer Institute of Chemical Technology for financial support. G.D. and J.P.B. gratefully acknowledge financial support from the Alexander von Humboldt Foundation (Bonn, Germany) for their respective Humboldt Research Fellowships. The current work was carried out with the support of the Karlsruhe Nano Micro Facility (KNMF), a Helmholtz Research Infrastructure at KIT. M. Glaßner is thanked for providing compound **2a**, R. Porter (Fraunhofer ICT, Pfinztal) for the contact-angle measurements, T. Tischer for assistance on the FT-IR microscope, and Dr. A. P. Vogt for photography. Finally, we thank Prof. Qing Lin and Dr. Zhipeng Yu for helpful discussions.

Received: September 2, 2011
Published online: November 17, 2011

[1] *Polymer Brushes: Synthesis, Characterization, Applications* (Eds: R. C. Advincula, W. J. Brittain, K. C. Caster, J. Rühe), Wiley-VCH, Weinheim, Germany **2004**.
[2] B. Zhao, W. J. Brittain, *Prog. Polym. Sci.* **2000**, *25*, 677.
[3] L. Nebhani, D. Schmiedl, L. Barner, C. Barner-Kowollik, *Adv. Funct. Mater.* **2010**, *20*, 2010.
[4] a) W. A. Braunecker, K. Matyjaszewski, *Prog. Polym. Sci.* **2007**, *32*, 93; b) A. D. Jenkins, R. G. Jones, G. Moad, *Pure Appl. Chem.* **2010**, *82*, 483.
[5] a) D. H. Solomon, E. Rizzardo, P. Cacioli; *EP135280* **1985**; b) D. H. Solomon, E. Rizzardo, P. Cacioli*Chem. Abstr.* **1985**, *102*, 221335q; c) C. J. Hawker, A. W. Bosman, E. Harth, *Chem. Rev.* **2001**, *101*, 3661.
[6] a) M. Kamigaito, T. Ando, M. Sawamoto, *Chem. Rev.* **2001**, *101*, 3689; b) K. Matyjaszewski, J. Xia, *Chem. Rev.* **2001**, *101*, 2921.
[7] a) *Handbook of RAFT Polymerization* (Ed: C. Barner-Kowollik), Wiley-VCH, Weinheim, Germany **2008**; b) G. Moad, E. Rizzardo, S. H. Tang, *Aust. J. Chem.* **2005**, *58*, 379; c) G. Moad, E. Rizzardo, S. H. Tang, *Aust. J. Chem.* **2006**, *59*, 669; d) G. Moad, E. Rizzardo, S. H. Tang, *Aust. J. Chem.* **2009**, *62*, 1402.
[8] a) H. C. Kolb, M. G. Finn, K. B. Sharpless, *Angew. Chem. Int. Ed.* **2001**, *40*, 2004; b) C. Barner-Kowollik, F. E. Du Prez, P. Espeel, C. J. Hawker, T. Junkers, H. Schlaad, W. Van Camp, *Angew. Chem. Int. Ed.* **2011**, *50*, 60.
[9] a) C. J. Hawker, K. L. Wooley, *Science* **2005**, *309*, 1200; b) W. H. Binder, R. Sachsenhofer, *Macromol. Rapid Commun.* **2007**, *28*, 15; c) C. Barner-Kowollik, A. J. Inglis, *Macromol. Chem. Phys.* **2009**, *210*, 987; d) R. K. Iha, K. L. Wooley, A. N. Nystrom, D. J. Burke, M. J. Kade, C. J. Hawker, *Chem. Rev.* **2009**, *109*, 5620; e) P. L. Golas, K. Matyjaszewski, *Chem. Soc. Rev.* **2010**, *39*, 1338.
[10] a) R. A. Evans, *Aus. J. Chem.* **2007**, *60*, 384; b) S. Sinnwell, A. J. Inglis, M. H. Stenzel, C. Barner-Kowollik, in *Click Chemistry for Biotechnology and Materials Science* (Ed: J. Lahann), Wiley, Chichester, UK **2009**, Ch. 6; c) H. Nandivada, J. Lahann, in *Click Chemistry for Biotechnology and Materials Science* (Ed: J. Lahann), Wiley, Chichester, UK **2009**, Ch. 12; d) A. J. Inglis, C. Barner-Kowollik, *Macromol. Rapid Commun.* **2010**, *31*, 1247; e) U. Mansfeld, C. Pietsch, R. Hoogenboom, C. R. Becer, U. S. Schubert, *Polym. Chem.* **2010**, *1*, 1560.
[11] a) S. Luza, H. Speisky, *Am. J. Clin. Nutr.* **1996**, *63*, 812S; b) F. Wolbers, P. ter Braak, S. Le Gac, R. Luttge, H. Andersson, I. Vermes, A. van den Berg, *Electrophoresis* **2006**, *27*, 5073; c) E. M. Sletten, C. R. Bertozzi, *Angew. Chem. Int. Ed.* **2009**, *48*, 6974.
[12] a) C. R. Becer, R. Hoogenboom, U. S. Schubert, *Angew. Chem. Int. Ed.* **2009**, *48*, 4900; b) J. T. Kopping, Z. P. Tolstyka, H. D. Maynard, *Macromolecules* **2007**, *40*, 8593; c) A. J. Inglis, S. Sinnwell, M. H. Stenzel, C. Barner-Kowollik, *Angew. Chem. Int. Ed.* **2009**, *48*, 2411; d) C. Ott, R. Hoogenboom, U. S. Schubert, *Chem. Commun.* **2008**, 3516; e) I. Singh, Z. Zarafshani, J.-F. Lutz, F. Heaney, *Macromolecules* **2009**, *42*, 5411; f) J. Moraes, T. Maschmeyer, S. Perrier, *J. Polym. Sci., Part A: Polym. Chem.* **2011**, *49*, 2771; g) C. F. Hansell, P. Espeel, M. M. Stamenovic, I. A. Barker, A. P. Dove, F. E. Du Prez, R. K. O'Reilly, *J. Am. Chem. Soc.* **2011**, *133*, 13828; h) M. Conradi, T. Junkers, *Macromolecules* **2011**, 44, 7969.
[13] a) C. E. Hoyle, C. N. Bowman, *Angew. Chem. Int. Ed.* **2010**, *49*, 1540; b) R. Hoogenboom, *Angew. Chem. Int. Ed.* **2010**, *49*, 3415; c) C. E. Hoyle, A. B. Lowe, C. N. Bowman, *Chem. Soc. Rev.* **2010**, *39*, 1355.
[14] a) T. Gruendling, K. K. Oehlenschlaeger, E. Frick, M. Glassner, C. Schmid, C. Barner-Kowollik, *Macromol. Rapid Commun.* **2011**, *32*, 807; b) M. Glassner, K. K. Oehlenschlaeger, T. Gruendling, C. Barner-Kowollik, *Macromolecules* **2011**, *44*, 4681.
[15] a) Y. Wang, C. I. Rivera Vera, Q. Lin, *Org. Lett.* **2007**, *9*, 4155; b) Y. Wang, W. J. Hu, W. Song, R. K. V. Lim, Q. Lin, *Org. Lett.* **2008**, *10*, 3725; c) W. Song, Y. Wang, J. Qu, M. M. Madden, Q. Lin, *Angew. Chem. Int. Ed.* **2008**, *47*, 2832.
[16] J. S. Clovis, A. Eckell, R. Huisgen, R. Sustmann, *Chem. Ber.* **1967**, *100*, 60.
[17] a) H. Meier, H. Heimgartner, *Helv. Chim. Acta* **1985**, *68*, 1283; b) V. Lohse, P. Leihkauf, C. Csongar, G. Tomaschewski, *J. Prakt. Chem.* **1988**, *330*, 406; c) R. Darkow, M. Yoshikawa, T. Kitao, G. Tomaschewski, J. Schellenberg, *J. Polym. Sci., Part A: Polym. Chem.* **1994**, *32*, 1657.
[18] a) G. Bertrand, C. Wentrup, *Angew. Chem. Int. Ed.* **1994**, *33*, 527; b) D. Moderhack, *J. Prakt. Chem.* **1998**, *340*, 687.
[19] J. Wang, W. Zhang, W. Song, Y. Wang, Z. Yu, J. Li, M. Wu, L. Wang, J. Zang, Q. Lin, *J. Am. Chem. Soc.* **2010**, *132*, 14812.
[20] a) W. Song, Y. Wang, J. Qu, Q. Lin, *J. Am. Chem. Soc.* **2008**, *130*, 9654; b) Y. Wang, W. Song, W. Hu, Q. Lin, *Angew. Chem. Int. Ed.* **2009**, *48*, 5330.
[21] M. M. Madden, C. I. Rivera Vera, W. Song, Q. Lin, *Chem. Commun.* **2009**, 5588.
[22] a) Z. Yu, R. K. V. Lim, Q. Lin, *Chem.-Eur. J.* **2010**, *16*, 13325; b) R. K. V. Lim, Q. Lin, *Acc. Chem. Res.* **2011**, in press, DOI: 10.1021/ar200021p; c) Z. Yu, L. Y. Ho, Z. Wang, Q. Lin, *Bioorg. Med. Chem. Lett.* **2011**, 21, 5033.
[23] G. Mantovani, F. Lecolley, L. Tao, D. M. Haddleton, J. Clerx, J. J. L. M. Cornelissen, K. Velonia, *J. Am. Chem. Soc.* **2005**, *127*, 2966.

[24] A. Wagner, C.-W. Schellhammer, S. Petersen, *Angew. Chem.* **1966**, *5*, 699.
[25] E. H. Lock, D. Y. Petrovykh, P. Mack, T. Carney, R. G. White, S. G. Walton, R. F. Fernsler, *Langmuir* **2010**, *26*, 8857.
[26] C. De Marco, S. M. Eaton, R. Suriano, S. Turri, M. Levi, R. Ramponi, G. Cerullo, R. Osellame, *ACS Appl. Mater. Interfaces* **2010**, *2*, 2377.
[27] E. Szocs, I. Bakó, T. Kosztolányi, I. Bertóti, E. Kálmán, *Electrochim. Acta* **2004**, *49*, 1371.
[28] P. G. Rouxhet, A. M. Misselyn-Bauduin, F. Ahimou, M. J. Genet, Y. Adriaensen, T. Desille, P. Bodson, C. Deroanne, *Surf. Interface Anal.* **2008**, *40*, 718.
[29] a) H. Meier, W. Heinzelmann, H. Heimgartner, *Chimia* **1980**, *34*, 506; b) S.-L. Zheng, Y. Wang, Z. Yu, Q. Lin, P. Coppens, *J. Am. Chem. Soc.* **2009**, *131*, 18036.
[30] D. Léonard, Y. Chevolot, O. Bucher, H. Sigrist, H. J. Mathieu, *Surf. Interface Anal.* **1998**, *26*, 783.
[31] D. Klemm, B. Heublein, H.-P. Fink, A. Bohn, *Angew. Chem. Int. Ed.* **2005**, *44*, 3358.
[32] J. S. Stevens, S. L. M. Schroeder, *Surf. Interface Anal.* **2009**, *41*, 453.
[33] A. S. Goldmann, T. Tischer, L. Barner, M. Bruns, C. Barner-Kowollik, *Biomacromolecules* **2011**, *12*, 1137.
[34] H. Murata, R. R. Koepsel, K. Matyjaszewski, A. J. Russell, *Biomaterials* **2007**, *28*, 4870.
[35] H. A. Krässig, in *Cellulose and Its Derivatives: Chemistry, Biochemistry and Applications* (Eds: J. F. Kennedy, G. O. Phillips, D. J. Wedlock, P. A. Williams), Ellis Horwood, Ltd., Chichester, UK **1985**, Ch. 1.
[36] K. L. Parry, A. G. Shard, R. D. Short, R. G. White, J. D. Whittle, A. Wright, *Surf. Interface Anal.* **2006**, *38*, 1497.
[37] J. H. Scofield, *J. Electron Spectrosc. Relat. Phenom.* **1976**, *8*, 129.
[38] S. Tanuma, C. J. Powell, D. R. Penn, *Surf. Interface Anal.* **1994**, *21*, 165.